All polarization-maintaining passively mode-locked fiber-ring ytterbium-doped laser; from net-normal to net-anomalous dispersion

C. Cuadrado-Laborde[1, 2, 3, *] *, A. Carrascosa[1], A. Díez[1], J. L. Cruz[1] and M. V. Andrés[1]

[1]*Departamento de Física Aplicada, ICMUV, Universidad de Valencia, Dr. Moliner 50, Burjassot E-46100, Spain*

[2]*Instituto de Física Rosario (CONICET-UNR), Blvr. 27 de Febrero 210bis, S2000EZP, Rosario, Argentina,*

[3]*Pontificia Universidad Católica Argentina, Facultad de Química e Ingeniería, Av. Pellegrini 3314, 2000, Rosario, Argentina*

**Corresponding author: christian.cuadrado@uv.es*

Abstract: We investigated the behavior of a fiber-ring polarization-maintaining passively mode-locked ytterbium-doped laser in a broad range of dispersion values; i.e., from highly net-normal to net-anomalous, with a special emphasis near the zero of chromatic dispersion. Different lengths of an *ad hoc* polarization-maintaining photonic crystal fiber were used as intracavity dispersion compensator to shift the operation of this laser from net-normal to the net-anomalous regime. The laser generated the shortest light pulses around the zero of dispersion: 6 ps / 7ps for −0.023 ps^2 / 0.045 ps^2; in both cases, pulses were not transform-limited, being theoretically possible an out-of-cavity recompression down to 170 fs / 220 fs, respectively. In the net-normal regime, we obtained a stable, ultra-low frequency, emission at 1.19 MHz, with pulses with a FWHM of 162 ps and pulse energy of 115 pJ. This laser presents a somewhat symmetrical behavior at both sides of the zero of dispersion thanks to its simple filter-free configuration. The laser is also environmentally robust, insensitive against temperature variations and mechanical vibrations, due to its integrated all-polarization-maintaining design.

Index Terms: fiber laser, ytterbium, mode-locking, polarization maintaining, photonic crystal fibers.

1. Introduction

The soliton-like formation is due to the interplay between the anomalous cavity dispersion and the fiber nonlinear optical Kerr effect [1, 2]; whereas in the net-normal dispersion regime, the soliton formation is a result of a complex balance among the normal cavity dispersion, fiber nonlinear Kerr effect, medium gain and losses [3, 4]. Therefore, and with the purpose to emphasize its different nature, the latter is known as a dissipative soliton. Determined by their different soliton shaping mechanisms, the solitons obtained have different features: while a soliton-like is transform-limited, a dissipative soliton is not. Notwithstanding, in the later, an out-of-cavity compression back to the transform-limit is also possible since the acquired extra-chirp is generally linear.

It is known that spectral filtering plays a key role in the genesis and stability of dissipative solitons; where the spectral filter is used to cut off the field at the end of each roundtrip so as to compensate for the large dispersion-induced positive chirp acquired during the roundtrip [5, 6, 7]. In soliton-like formation, spectral filtering has a key role also [8, 9]. However, this is to some extent forgotten by the fact that most proposals naturally fall where standard fibers present the required anomalous dispersion; i.e., above 1.3 μm. Above that

wavelength, erbium is the common choice as a gain medium, whose narrow band performs this task in the form of a gain frequency filtering. On the contrary, when a fiber cavity is deliberatively designed to work in the soliton-like regime below 1.3 μm, it is necessary not only to provide artificially a mechanism to shift the average dispersion from net-normal to net-anomalous –see [10], and references therein– but also some kind of frequency limiter, since ytterbium as a gain medium cannot perform this task, due to its broadband emission characteristics. An interesting solution to this trade-off was to take advantage of the possibilities offered by ytterbium-doped photonic crystal fibers in its different variations, which simultaneously provide gain, dispersion compensation, and spectral filtering, in a single element. Thus, different soliton-like fiber lasers below 1.3 μm have been proposed by using a suspended-core ytterbium-doped silica fiber [11], or a ytterbium-doped photonic bandgap fiber [12]. However, these proposals were not demonstrated in a true polarization-maintaining cavity, or even included free-space optics.

Nevertheless, there are important requirements that any fiber laser should fulfill for out-of-laboratory applications, among them: robustness against environmental fluctuations, turnkey operation, cost effectiveness, and simplicity. Some of these requirements leave out of the equation those proposals relying on free-space optics or with intracavity moving components. Further, for some applications, it is required immunity against harsh environments, where thermal and mechanical stresses decidedly influence the birefringence properties of fiber cavities, eventually degrading the laser performance or even precluding at all its operation. On the contrary, a fiber cavity entirely constructed out of polarization-maintaining (PM) fibers and PM components avoid these inconveniences. This is the reason why all in-fiber PM solutions have deserved an increasing attention over the last few years. However, in doing so, this precludes also the possibility to use the polarization evolution within the cavity as an additional degree of freedom to stabilize the laser. In a few words, and in opposition to non-PM solutions, once a full in-fiber PM laser is assembled, the only parameter that can be varied to stabilize the laser is the pump power. Of course, this is the main strength of a PM all-fiber laser, but at the same time, it demands from designers a more precise knowledge on the subject under study. A few works have analyzed the influence of dispersion in the behavior of a mode-locked fiber laser, spanning from the net-normal to the net-anomalous regimes. Among them, Zhang et al. studied the behavior of a single ytterbium-doped passively mode-locked fiber laser, using a chirped fiber Bragg grating for dispersion management; depending on its orientation, the cavity presents a highly normal or highly anomalous dispersion [13]. In each configuration, the cavity delivered dissipative solitons and soliton-like pulses, helped by the narrow bandwidth of the chirped fiber grating used [12]. A previous theoretical work by Kalosha et al. arrived to similar results [14]. It is worth to remark that in these proposals the polarization preservation was not taken into account.

Here, we study the behavior of a fiber-ring fully polarization-maintaining passively mode-locked ytterbium-doped laser under a broad range of dispersion values, ranging from net-normal to net-anomalous, with a special emphasis near the zero of dispersion. Different lengths of an *ad hoc* polarization-maintaining photonic crystal fiber were used as intracavity dispersion compensator to shift the operation of this laser from net-normal to the net-anomalous regime. Further, with the purpose to give one step forward in the simplification of these lasers, we have studied its behavior when the filtering action is solely performed from the intrinsic broadband of the active fiber. This simplified all-in-fiber polarization-maintaining ytterbium-doped laser was characterized in detail in both regimes: net-normal and net-anomalous.

2. Experimental Details

A schematic diagram of the mode-locked laser is illustrated in Fig. 1(a); the laser operates in a fiber ring configuration. The gain was provided by 0.47 m long PM ytterbium highly-doped, single-clad, optical fiber (PM YDF) (YDF-SM-6/125 panda clad shape by NOVAE, core absorption > 700 dB/m at 975 nm, and numerical aperture of 0.16 $\pm$ 0.02). The PM YDF was pumped through a polarization-maintaining wavelength division multiplexer (PM

WDM, 980 nm/1060 nm) by a 976 nm emission wavelength pigtailed laser diode, providing a maximum pump power of 500 mW. Next, at the output of the PM YDF was sandwiched a saturable absorber in transmission (SA) (BATOP GmbH, high reflection band 1050 nm ≤ λ ≤ 1090 nm, relaxation time constant 500 fs, absorptance 35 %, modulation depth 13 %, and saturation fluence of 300 μJ/cm^2) between two standard FC-PC fiber connectors, in order to guarantee the all-fiber structure of the laser. We decide to use a SA as mode-locker, because its saturable absorption is independent of cavity length. At the output of the SA was fusion-spliced the input of a polarization-maintaining optical isolator (PM ISO) (center wavelength 1064 nm, fast axis blocked, > 22 dB extinction ratio). In turn, the output of the PM ISO was fusion-spliced to the input of a 80/20 polarization-maintaining optical fiber coupler (PM OFC). The fiber-ring cavity was closed by using a delay line, which was fusion spliced between the 80 % output of the PM OFC and the remaining port of the PM WDM. The output of this laser was obtained through the 20 % port of the PM OFC. The output light pulses were monitored by using a 60 GHz sampling oscilloscope provided with a fast built-in photodetector (53 GHz), real-time 2.5 GHz bandwidth oscilloscope, intensity autocorrelator (maximum scan range 200 ps), and optical spectrum analyzer (wavelength accuracy >20 pm). We finally emphasize the complete lack of a filter within the cavity; the filtering performance of the different components within the cavity should not be taken into account due to its broadband characteristics; as an example the measured −3 dB bandwidth of the PM OFC was 69 nm.

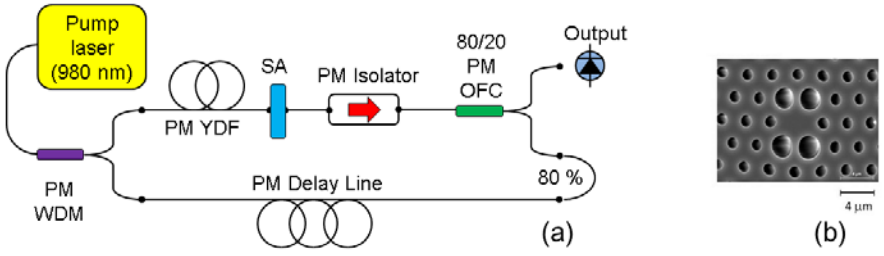

Fig. 1. (a) Experimental laser setup; where SA, OFC, and WDM stands for saturable absorber, optical fiber coupler, and wavelength division multiplexer, respectively. (b) Photograph taken with a scanning electron microscope showing a transversal slice of the polarization maintaining photonic crystal fiber used as delay line in some experiments.

The original configuration was with a PM YDF length of 0.47 m, and a PM SMF delay line length of 17.1 m (PM980-XP by Nufern, cut-off wavelength of 920 ± 50 nm, and numerical aperture of 0.120); this configuration of the cavity includes the pigtails of the PM fiber optics components (PM WDM, PM OFC, etc.), which all have the same characteristics of the PM SMF. We also investigated the behavior of our laser by modifying this delay line, not only in its length but in its composition also by using an *ad hoc* polarization-maintaining photonic crystal fiber (PM PCF), specially designed and fabricated in our facilities [15, 16]. Figure 1(b) shows a photograph of a transversal slice of the PM PCF by using a scanning electron microscopy; the strong geometrical anisotropy observed is ultimately responsible for the polarization maintenance. The presence of the delay line allows changing the net dispersion of the cavity from different values of net-normal to net-anomalous. Our study begins with a full characterization of the original configuration. Next, we experimentally analyzed the effect of a change of the net (normal) dispersion on the output light pulses, taking as starting point the original configuration. Therefore, we first progressively decreased the PM SMF length down to 1.77 m, and next progressively increasing the PM SMF length up to 172 m; while simultaneously keeping fix the PM YDF. Finally, we also shifted the net dispersion of the cavity from net-normal to net-anomalous, by replacing the PM SMF of the delay line with different lengths of a PM PCF.

The chromatic dispersions of both the PM SMF and the PM PCF were measured in our laboratory by the interferometric technique [17] resulting in 24 ps^2/km, and −9 ps^2/km, respectively, at 1030 nm; whereas we estimated the dispersion of the PM YDF was of 25

ps^2/km. On the other hand, the power loses during each round trip of the light pulses were not significant, which is one of the main advantages of a full in-fiber configuration. By taking as starting point the SA, see Fig. 1(a), and in a clockwise direction, the discrete power loses within the cavity were: –0.4 dB (insertion loss of the SESAM), –1.5 dB (insertion loss of the PM ISO), –0.97 dB (80 % output of PM OFC), and –0.7 dB (insertion loss of PM WDM); this is below 3.6 dB of discrete power losses during each round-trip. To this total discrete power loss should be added the distributed power loses provided by the PM YDF (< 10 dB/km at 1100 nm) plus either PM SMF or PM PCF, with <2.5 dB/km and <120 dB/km, respectively. Further, in the last case, it should also be taken into account that the fusion-splicing of a PM PCF with a standard PM SMF is not a trivial task, due to the inherent numerical aperture mismatch, giving typically a measured power loss of –1.5 dB. Therefore, the total combined discrete-distributed power losses within one round-trip were below 4 dB and 6.7 dB, when either PM SMF or PM PCF, respectively, was used as delay line.

3. Results and Discussion

In the following, we will characterize the original all-normal dispersion (ANDi) configuration. Next, we will study the changes in the output light pulses of this laser when the net dispersion of this cavity spans from high net-normal values of chromatic dispersion to net-anomalous, with a special emphasis in the behavior around the zero of dispersion.

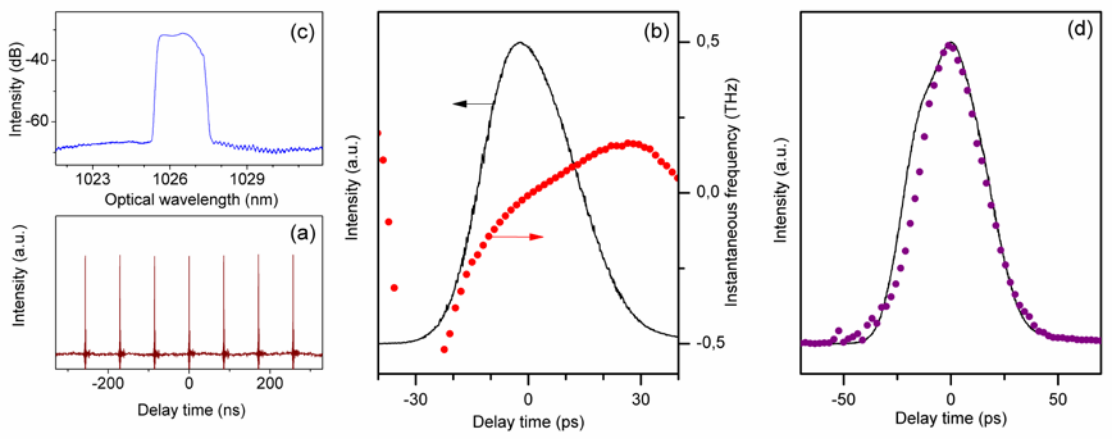

Fig. 2. (a) Temporal trace of the output light train. (b) Temporal waveform of one single pulse –left axis– and its corresponding instantaneous frequency profile –right axis– (solid curve and solid scatter points, respectively). (c) Output light pulse spectrum. (d) Temporal waveform at the output of the dispersive delay line used to obtain the instantaneous frequency profile together with a simulated propagated pulse, whose phase profile was retrieved by using the instantaneous frequency profile shown in 2(b) (solid curve and solid scatter points, respectively).

The laser was self-starting for all configurations once the pump power reaches the required level, being unnecessary any mechanical perturbation to initiate mode-locking. In each case, we monitored the pulse waveform, spectrum, and intensity autocorrelation trace (in this case, only whenever the measured light pulses fall below the resolution limit of our sampling oscilloscope). As it was appointed above in Section 2, the original configuration consists of 0.47 m length of PM YDF and a delay line length of 17.1 m PM SMF– which also includes all pigtails of the PM fiber optics components, resulting in a total cavity length of 17.57 m. As a result, the cavity presents a moderately high net-normal dispersion of 0.44 ps^2. Figure 2(a) shows the output light pulses train at a frequency of 11.67 MHz for a pump power of 108 mW; as expected, the measured frequency corresponds well with the reciprocal of the round-trip time for the measured cavity length. The output light pulse train of this laser showed good stability for all the series of experiments performed in this work, once the appropriate

pump power range was found. In this specific case, with a standard deviation in intensity below 1 %, and a measured timing jitter < 1 ps. In Fig. 2(b) we show the temporal intensity profile of a single light pulse, with an FWHM of 27 ps and a measured peak power of 0.784 W (pulse energy of 21.2 pJ). On the other hand, the spectrum of the output light pulses is shown in Fig. 2(c); without any filtering within the cavity, the laser emits at the central optical wavelength of 1026.51 nm, with an optical bandwidth of 1.45 nm / 2.1 nm (either by measuring at –3 dB or –10 dB, respectively). Since the cavity is entirely ANDi, this laser operates at the dissipative soliton regime, as confirmed by the steep spectral edges in the optical spectrum. The time-bandwidth product (TBP) in this case is between 11 and 16, well above the TBP of ~0.315 for a transform-limited $sech^2$ pulse, showing that these mode-locked pulses are highly chirped [18, 19], which also is a typical signature of the dissipative soliton regime. Therefore, these chirped light pulses could be recompressed up to the limit given by the time-bandwidth product: ~0.5 ps.

Next, we measured the instantaneous frequency (IF) profile of the output light pulses by using a simple technique previously developed by us [20, 21, 22]. The technique only requires measuring the temporal intensity waveforms at the input and output of a dispersive line –in this case: 160 m length of PM SMF–, together with the knowledge of the chromatic dispersion of the optical fiber. Therefore, the IF profile is obtained just by using a single equation in a non-iterative single-step numerical calculation which is shown on the right axis in Fig. 2(b). There, we can observe, in the central section of the light pulse, a linear chirp with a slope of 8.8 GHz/ps. We decided to test the IF profile obtained, by simulating the propagation of a numerically assembled input light pulse through the same dispersive line used to retrieve the IF profile. Where the amplitude of this signal was given by the square root of the measured temporal intensity, and its temporal phase, by numerical integration of the IF profile; both shown in Fig. 2(b). We show in Fig. 2(d) both the measured temporal waveform at the output of the dispersive line, together with the simulated output; there is a reasonable degree of resemblance between both, which could be improved by using a short delay line in the retrieval of the IF profile [20].

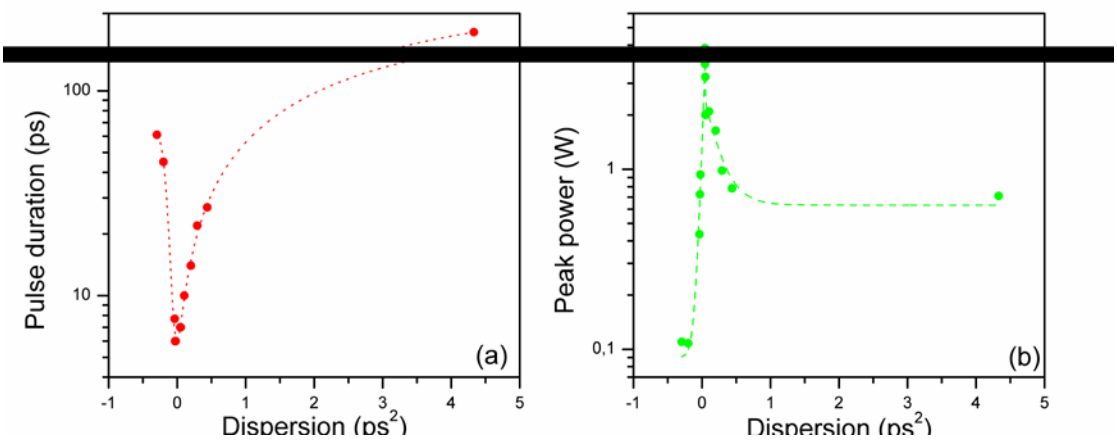

Fig. 3. Pulse duration and peak power –both in a logarithmic scale– as a function of cavity dispersion, (a) and (b) respectively. In both cases, the dashed curves are just a guide to the eyes.

Then, and by taking as a reference to the original configuration, we progressively varied the length of the optical fiber cavity by adding/subtracting PM SMF; in order to remain always in the net-normal regime. Thus, the total cavity length varied from a minimum of 1.77 m up to a maximum of 172.5 m; therefore, the net (normal) dispersion of the cavity ranged between 0.045 ps^2 and 4.33 ps^2; i.e., a variation of two orders of magnitude. Of course, this

was accompanied with a reciprocal frequency change in the output light pulse train from 115.2 MHz up to 1.19 MHz. Further, driving the laser at the lowest frequency (1.19 MHz) requires a careful procedure, which is otherwise not necessary at higher frequencies. Thus, when we have an ultra-long cavity, and once the pump power is raised enough, the laser spontaneously emits in the multipulsing regime. However, even in this case, it is possible to reach a single pulse emission by very slowly reducing the pump power until the required level (98 mW in this case). Once this single pulse emission regime is obtained, the pump power can be raised up to 27 % without multi-pulsing; thus showcasing the emission a strong hysteresis as a function of pump power. Also, we were able to reverse the net dispersion sign of the cavity, by using a delay line made of different lengths of an *ad hoc* PM PCF, which provided enough anomalous chromatic dispersion at the emission wavelength of this laser. Thus, we also studied the behavior of this laser when the net-anomalous chromatic dispersion ranged between -0.023 ps^2 and -0.296 ps^2. In this regime, we did not observe soliton mode-locking; notwithstanding, according to a previous theoretical study [8], a self-starting and stable emission of solitons requires of both, a saturable absorber and a frequency limiter. While the former sculpts the pulse in the time domain, the later do it in the Fourier's domain. It is true that in some setups these devices are not explicitly presents [23, 24], but even in that case, it can be demonstrated that they were implicitly included. One example of each case can illustrate this point further, a birefringent optical fiber sandwiched between two polarization-selective elements behaves as a saturable absorber [25, 26], and the presence of an element with strong wavelength-dependent losses –like a photonic bandgap fiber– can serve as frequency limiter [24, 11]. In our setup there is a SA, but neither explicitly, nor implicitly, a frequency limiter. Further, gain filtering is frequently used as an implicit frequency limiter at 1.5 μm, due to the narrow emission bandwidth in erbium. However, this option can be discarded at 1 μm, due to the broad emission bandwidth of ytterbium.

Figures 3(a) and 3(b) show the pulse duration and peak power, respectively, as a function of dispersion. In Fig. 3(a), we observe how the pulse duration monotonically decreases when the magnitude –i.e., the absolute value– of the chromatic dispersion approaches zero, although with slightly different rates, being slower in the net-normal dispersion regime. In Ref. [14], Kalosha and coworkers numerically study a passively modelocked –via the use of a saturable absorber– ANDi fiber laser, which also includes an intra-cavity PCF for dispersion compensation; which allows them the possibility to span from net-normal to net-anomalous dispersion regimes, exactly as we have done experimentally in this work. Our experimental results –showed in Fig. 3(a)– follows exactly the same trend as reported by them. Much more recently, Zhang et al. arrived to similar results, by using a chirped fiber Bragg grating for dispersion management, therefore the cavity net dispersion could be changed from largely normal (2.4 ps^2) to largely anomalous (-2.0 ps^2), just changing the orientation of the chirped Bragg grating within the laser cavity [13]. Both works [13, 14] have in common the use of a frequency limiter within the cavity; as a consequence, transform-limited solitons were obtained in the net-anomalous regime. The peak power, which is shown in Fig. 3(b), shows the complementary trend as compared with the pulse duration shown in Fig. 3(a), with peak powers up to 4 W for the shortest pulses (~6 ps), and monotonically decreasing at both sides of the zero of dispersion, although at a much faster rate in the net-anomalous dispersion regime. These results implied pulses energies ranging from 27 pJ (7 ps) to 115 pJ (162 ps) and 6 pJ (6 ps) to 7 pJ (61 ps), in the net-normal and net-anomalous regimes, respectively. Further, in the lowest frequency of the net-normal regime, the measured energy is in accordance with previously reported works [27]. The necessary pump powers to reach a steady state emission are shown in Fig. 4(a); as we approach the zero of

dispersion, the higher the pump power required. In the net-anomalous regime, this is a consequence of the non-soliton-like emission, since pump powers in this emission regime are generally lower. On the other hand, Fig. 4(b) shows the spectral width, as a function of the net dispersion of the cavity; whereas in the Fig. 4(c) we show three different representative spectra of both regimes: net-normal and net-anomalous. In the net anomalous regime, the spectra are broad and typically Gaussian; as it was appointed before, we did not observe transform-limited soliton pulses at net-anomalous dispersion, which was rubricated not only by the absence of Kelly sidebands in the measured spectra but also by the high TBP (= 139); these light pulses could be recompressed out of the cavity up to ~130 fs. In the net-normal regime they showed a stepped profile, which is typical of ANDi lasers. This monotonically decreasing spectral bandwidth with increasing net-normal dispersion follows the same trend reported in the systematic numerical study of Chong et al. for ANDi fiber lasers [28]; which was further experimentally corroborated later [13]. Interestingly, Chong et al. found that decreasing the net-normal dispersion produces a trend in the spectral profile that is similar to those obtained by increasing the nonlinear phase change or decreasing the intracavity filter bandwidth [28].

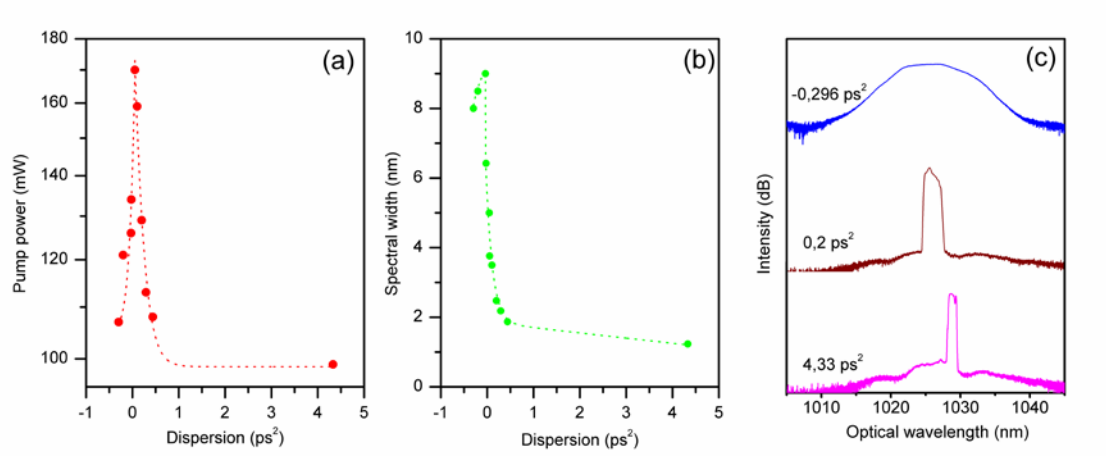

Fig. 4. Pump power and spectral width as a function of dispersion, (a) and (b) respectively. In both cases the dashed curves are just a guide to the eyes. (c) Three different spectral profiles at the following values of net dispersion: –0.296 ps^2, 0.2 ps^2, and 4.33 ps^2.

When an ANDi fiber cavity is lengthened, this may lead to the enhancement of nonlinear optical effects. These accumulated nonlinearities may play a detrimental role, resulting in total destabilization of the laser output toward a regime in which the output pulse train consists of irregular bursts with intense fluctuations; i.e., noise-like pulses (NLP) [29]. NLPs have a broadband spectrum, but its more distinctive signature is given by the autocorrelation trace, which consists of a broad background with a sharp narrow central peak [30]. With the purpose to elucidate this point, we also performed autocorrelation measurements in both regimes of our laser; i.e., under net-normal and net-anomalous chromatic dispersion. We show merely as an example in Fig. 5(a) and 5(b), respectively, the autocorrelation traces of the output light pulses for the original configuration (net-normal chromatic dispersion within the cavity of +0.2 ps^2) and when the intracavity delay line was made entirely of PM PCF (net-anomalous chromatic dispersion within the cavity of –0.2 ps^2). Neither in Fig. 5(a) nor 5(b), there is any trace corresponding with the emission of NLPs; being the measured pulses durations –via decorrelation– in correspondence with the values previously measured with the sampling oscilloscopes.

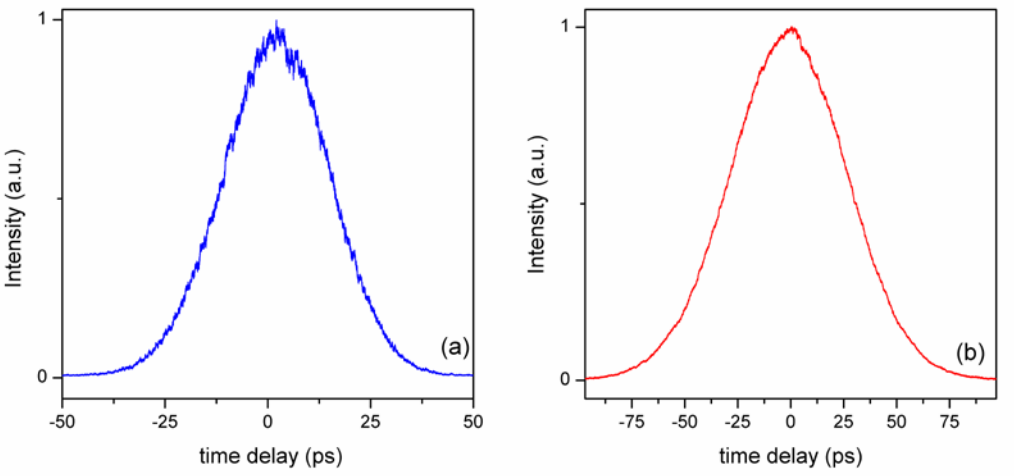

Fig. 5. Measured intensity autocorrelation traces of the output light pulses when the total cavity dispersion was net normal (+0.2 ps^2) and net-anomalous (–0.2 ps^2); figures (a) and (b), respectively.

4. Conclusions

We investigated the behavior of a filter-free polarization-maintaining fiber-ring passively mode-locked ytterbium-doped laser in a broad range of dispersion values: from highly net-normal to net-anomalous; with a special emphasis near the zero of dispersion. Different lengths of an *ad hoc* PM PCF were used as intracavity dispersion compensator to shift the operation of this laser to the net-anomalous regime. The laser generated the shortest light pulses around the zero of dispersion: 6 ps / 7ps for –0.023 ps^2 / 0.045 ps^2; in both cases, pulses were not transform-limited, being theoretically possible an out-of-cavity recompression down to 170 fs / 220 fs, respectively. In the net-normal regime, we obtained a stable, ultra-low frequency, emission at 1.19 MHz, with pulses with a FWHM of 162 ps and pulse energy of 115 pJ. Thanks to the integrated all-polarization-maintaining design, the laser is environmentally robust, insensitive against temperature variations and mechanical vibrations in the broad range of dispersion values under analysis.

Acknowledgements

This work has been financially supported by the *Agencia Estatal de Investigación* (AEI) of Spain and *Fondo Europeo de Desarrollo Regional* (FEDER) (Ref.: TEC2016-76664-C2-1-R) C. Cuadrado-Laborde acknowledges the financial support from project PICT 2015-1828 (FONCYT, Argentina), PIP 11220150100607CO (CONICET, Argentina) and the *Programa de Investigadores Invitados de la Universidad de Valencia* (Spain).

References

1 L.F. Mollenauer and R. H. Stolen, “The soliton laser,” Opt. Lett. 9, 13-15 (1984).

2 H. Haus and M. Islam, "Theory of the soliton laser," IEEE J. Quantum Elect. 21, 1172-1188 (1985).

3 A. Chong, J. Buckley, W. Renninger, and F. Wise, "All-normal-dispersion femtosecond fiber laser," Opt. Express 14, 10095-10100 (2006).

4 A. Chong, W.H. Renninger, and F.W. Wise, “All-normal-dispersion femtosecond fiber laser with pulse energy above 20nJ,” Opt. Lett. 32, 2408-2410 (2007).

5 J. Buckley, A. Chong, S. Zhou, W. Renninger, and F.W. Wise, “Stabilization of high-energy femtosecond ytterbium fiber lasers by use of a frequency filter,” J. Opt. Soc. Am. B. 24, 1803-1806 (2007).

6 B.G. Bale, J.N. Kutz, A. Chong, W.H. Renninger, and F.W. Wise, “Spectral filtering for mode locking in the normal dispersive regime,” Opt. Lett. 33, 941-943 (2008).

7 B.G. Bale, J.N. Kutz, A. Chong, W.H. Renninger, and F.W. Wise, “Spectral filtering for high-energy mode-locking in normal dispersion fiber lasers,” J. Opt. Soc. Am. B. 25, 1763-1770 (2008)

8 C.-J. Chen, P.K.A. Wai, and C.R. Menyuk, "Soliton fiber ring laser," Opt. Lett. 17, 417-419 (1992).

9 X. Zhang, F. Li, K. Nakkeeran, J. Yuan, Z. Kang, J. Nathan Kutz , and P.K.A. Wai, “Impact of Spectral Filtering on Multipulsing Instability in Mode-Locked Fiber Lasers,” IEEE J. Sel. Top. Quant. 24: 1101309 (2018).

10 L. Chen, J. Huynh., H. Zhou, M. Chyla, M. Smrž, and T, Mocek, “Generating 84 fs, 4 nJ directly from an Yb-doped fiber oscillator by optimization of the net dispersion,” Laser Phys. 29, 065105 (2019)

11 A. Chamorovskiy, Y. Chamorovskiy, I. Vorobev and O.G. Okhotnikov, "95-Femtosecond Suspended Core Ytterbium Fiber Laser," IEEE Photonic Tech. L. 22, 1321-1323, 2010.

12 A. Isomäki and O.G. Okhotnikov, "Femtosecond soliton mode-locked laser based on ytterbium-doped photonic bandgap fiber," Opt. Express 14, 9238-9243 (2006).

13 L. Zhang, A.R. El-Damak, Y. Feng, and X. Gu, "Experimental and numerical studies of mode-locked fiber laser with large normal and anomalous dispersion," Opt. Express 21, 12014-12021 (2013).

14 V.P. Kalosha, L. Chen, and X. Bao, “Ultra-short pulse operation of all-optical fiber passively mode-locked ytterbium laser,” Opt. Express 14, 4935-4945 (2006).

15 M. Delgado-Pinar, A. Diez, J.L. Cruz and M.V. Andres, “High Extinction-Ratio Polarizing Endlessly Single-Mode Photonic Crystal Fiber,” IEEE Photonics Tech. L. 19, 562-564 (2007).

16 M. Delgado-Pinar, A. Díez, S. Torres-Peiró, M.V. Andrés, T. Pinheiro-Ortega, and E. Silvestre, “Waveguiding properties of a photonic crystal fiber with a solid core surrounded by four large air holes,” Opt. Express 17, 6931-6938 (2009)

17 R.B. Dyott, Elliptical Fiber Waveguides (London: Artech House, 1995).

18 D.S. Kharenko, O.V. Shtyrina, I.A. Yarutkina, E.V. Podivilov, M.P. Fedoruk, and S.A. Babin, “Highly chirped dissipative solitons as a one-parameter family of stable solutions of the cubic–quintic Ginzburg–Landau equation,” J. Opt. Soc. Am. B 28, 2314-2319 (2011).

19 D.S. Kharenko, E.V. Podivilov, A.A. Apolonski, and S.A. Babin, “20 nJ 200 fs all-fiber highly chirped dissipative soliton oscillator,” Opt. Lett. 37, 4104-4106 (2012).

20 C. Cuadrado-Laborde, A. Carrascosa, P. Pérez-Millán, A. Díez, J.L. Cruz, and M.V. Andrés. "Phase recovery by using optical fiber dispersion," Opt. Lett. 39, 598-601 (2014).

21 C. Cuadrado-Laborde, M. Brotons-Gisbert, G. Serafino, A. Bogoni, P. Pérez-Millán, and M.V. Andrés. "Phase recovery by using optical fiber dispersion and pulse pre-stretching," Appl. Phys. B 117, 1173-1181 (2014).

22 C. Cuadrado-Laborde, I. Armas-Rivera, A. Carrascosa, E.A. Kuzin, A. Díez, and M.V. Andrés, "Instantaneous frequency measurement of dissipative soliton resonance light pulses" Opt. Lett. 41 5704-5707 (2016).

23 R. Herda, et al., "Environmentally Stable Mode-Locked Fiber Laser With Dispersion Compensation by Index-Guided Photonic Crystal Fiber," IEEE Phot. Tech. L. 20, 217-219, 2008.

24 X. Liu, J. Lægsgaard, and D. Turchinovich, "Self-stabilization of a mode-locked femtosecond fiber laser using a photonic bandgap fiber," Opt. Lett. 35, 913-915 (2010)

25 R.H. Stolen, J. Botineau, and A. Ashkin, "Intensity discrimination of optical pulses with birefringent fibers," Opt. Lett. 7, 512-514 (1982).

26 M.N. Islam, C.E. Soccolich, J.P. Gordon, and U.C. Paek, "Soliton intensity-dependent polarization rotation," Opt. Lett. 15, 21-23 (1990).

27 E.J.R. Kelleher, J.C. Travers, Z. Sun, A.G. Rozhin, A.C. Ferrari, S.V. Popov, and J.R. Taylor, “Nanosecond-pulse fiber lasers mode-locked with nanotubes,” Appl. Phys. Lett. 95:111108 (2009).

28 A. Chong, W.H. Renninger, and F.W. Wise, "Properties of normal-dispersion femtosecond fiber lasers," J. Opt. Soc. Am. B 25, 140-148 (2008).

29 M. Horowitz, Y. Barad, and Y. Silberberg, "Noiselike pulses with a broadband spectrum generated from an erbium-doped fiber laser," Opt. Lett. 22, 799-801 (1997).

30 C. Aguergaray, A. Runge, M. Erkintalo, and N. G. R. Broderick, "Raman-driven destabilization of mode-locked long cavity fiber lasers: fundamental limitations to energy scalability," Opt. Lett. 38, 2644-2646 (2013)